2007 11 15

1930 *Raman*

Raman

1930

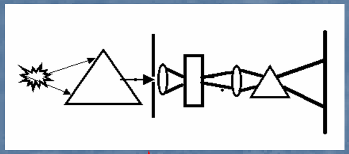

435.8 nm (Hg-line)

anti-Stokes Stokes

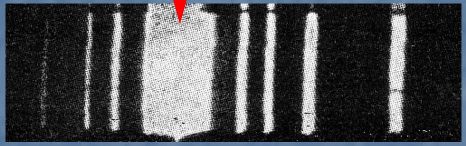

Resolution ca. 10 cm-1
Sample Volume: ca. 1 liter
Exposure time: ca. 40 hours

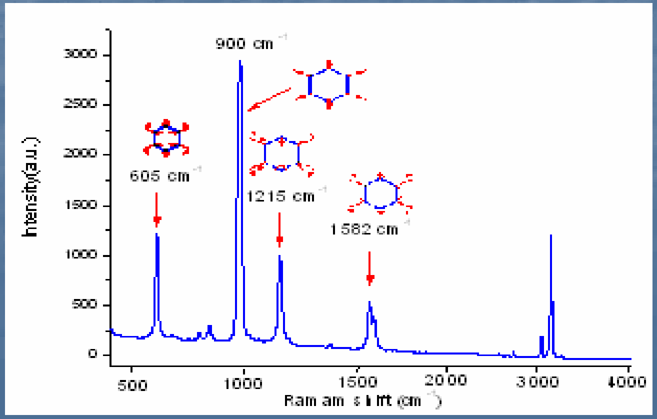

2007

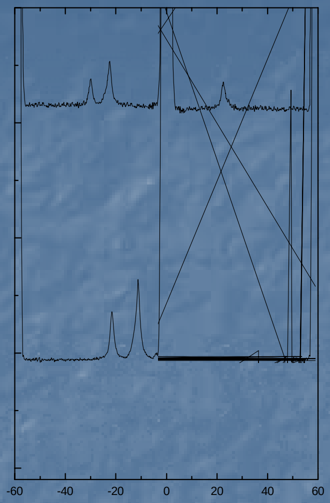

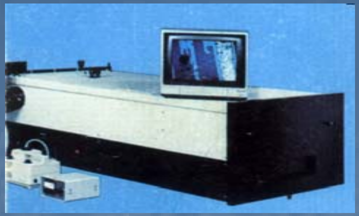

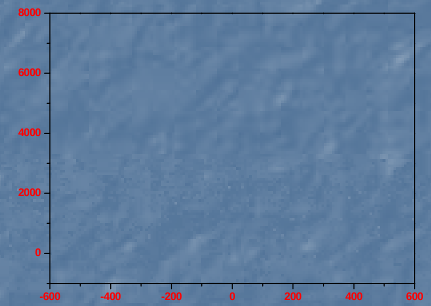

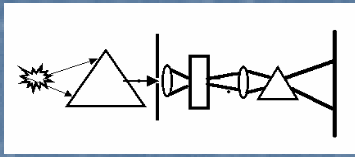

435.8 nm (Hg-line)

anti-Stokes Stokes

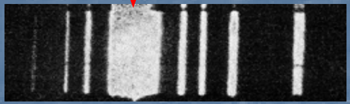

Resolution ca. 10 cm-1
Sample Volume: ca. 1 liter
Exposure time: ca. 40 hours

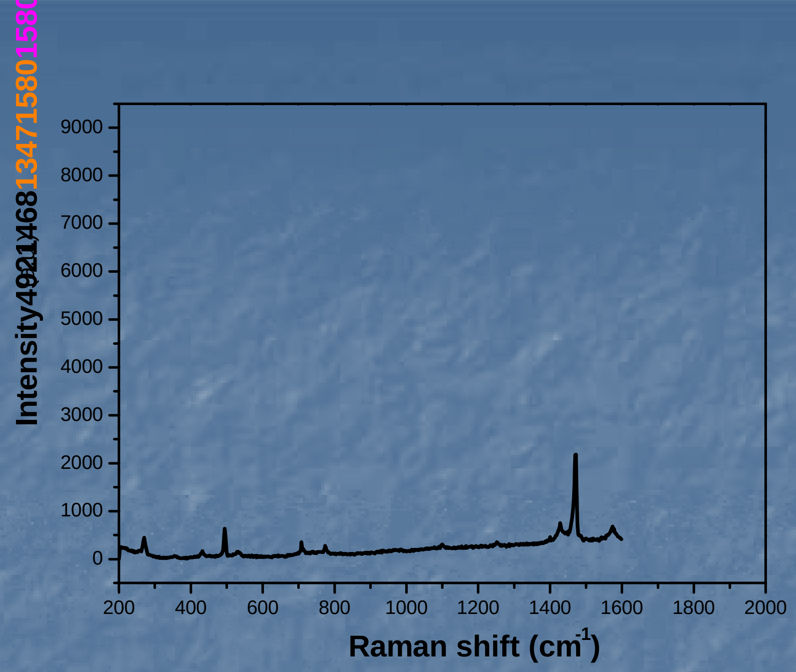

Intensity
9000
8000
7000
6000
5000
4000
3000
2000
1000
0
200
400
600
800
1000
1200
1400
1600
1800
2000
Raman shift (cm-1)

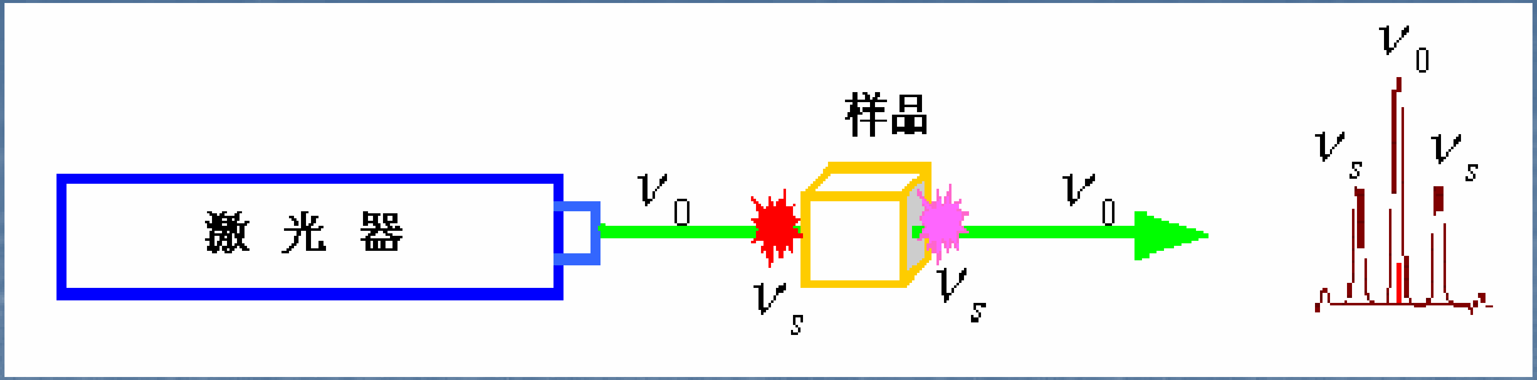

ν_0

ν_0

ν_0

ν_s

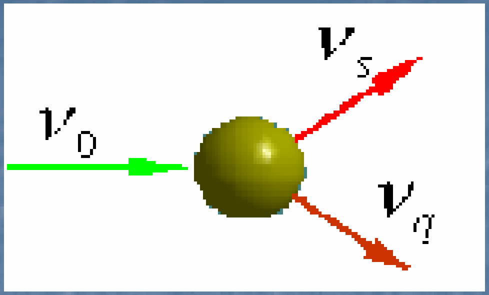

?

$h\nu_0$ hk_0

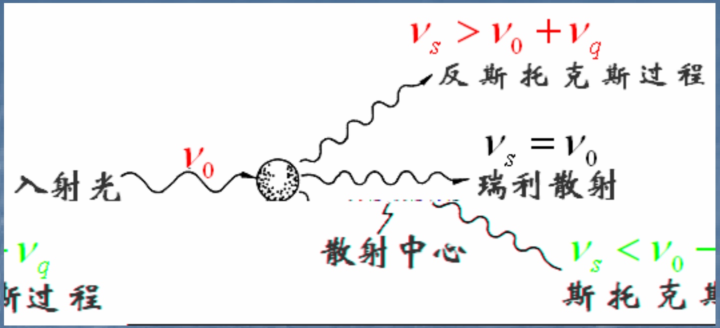

ν_s ν_0

Rayleigh $\nu_s < \nu_0$,

Stokes

$\nu_s > \nu_0$

Stokes

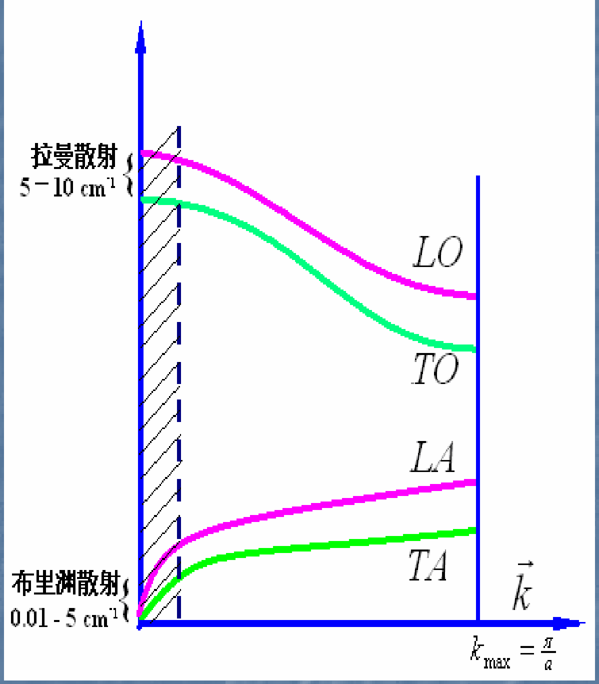

- 10－5000 cm^{-1}

- 0.01－2cm^{-1}

10^5 cm^{-1},

(10^8 cm^{-1})

1. 2. 3. 4. 5. 6.	*1.* , 2. *3.* /

(3.1)

$$E = E_0 \cos \omega_0 t$$ 3-1

E_0 ω_0

P

$$P = \alpha E = \alpha E_0 \cos \omega_0 t$$ 3-2

α

:

3-3
$$q = q_0 \cos \omega_q t$$

q_0

$$\alpha = \alpha_0 + (\frac{\partial \alpha}{\partial q})_0 q_0 + ...$$ 3-4

α_0

3-3 3-4 3-2

$$P = \alpha E_0 \cos \omega_0 t$$
$$= \alpha E_0 \cos \omega_0 t + (\frac{\partial \alpha}{\partial q})_0 q E_0 \cos \omega_0 t$$
$$= \alpha E_0 \cos \omega_0 t + (\frac{\partial \alpha}{\partial q})_0 q E_0 \cos \omega_0 t \cos \omega_q t$$ 3-5
$$= \alpha E_0 \cos 2\pi \nu_0 t + \frac{1}{2}(\frac{\partial \alpha}{\partial q})_0 q E_0 [\cos 2\pi(\nu_0 + \nu_q)t + \cos 2\pi(\nu_0 - \nu_q)t]$$

(3-5)

3 1

2 (ν_0+ ν_q) 3

(ν_0- ν_q) 3-5

(3-5)

$$\nu_s = \nu_0 - \nu_q$$

d d d

$$k_s = k_0 - k_q$$

$$\Delta\nu = \nu_0 - \nu_q$$

d d d

$$\Delta k = k_0 - k_q$$

3-6

Stokes

(3-5)

$$\nu_s = \nu_0 + \nu_q$$

d d d

$$k_s = k_0 + k_q$$

$$\Delta\nu = \nu_0 - \nu_q$$

d d d

$$\Delta k = k_0 - k_q$$

3-7

Stokes

3-6 **3-7** Stokes

3.2

$$|\vec{K}_s| \approx |\vec{K}_0|$$

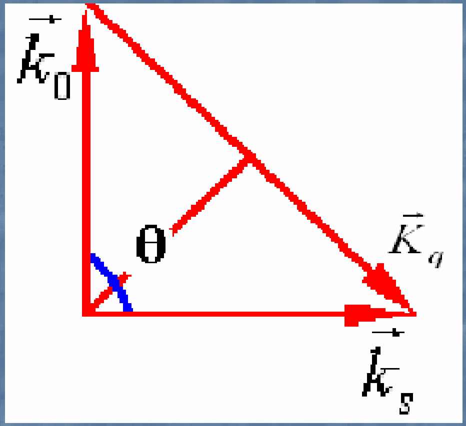

$$|k_q| = 2 \cdot |k_0| \cdot n \cdot \sin\frac{\theta}{2} \qquad 3\text{-}8$$

n θ

: $k_0(e_i^s e_j^0)k_s$

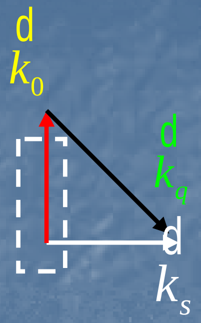

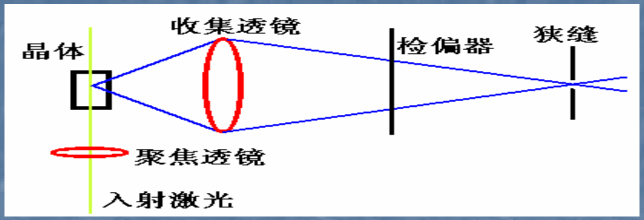

90 °

$x(zz)y; x(zx)y; x(xx)y; x(yx)y$

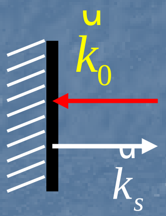

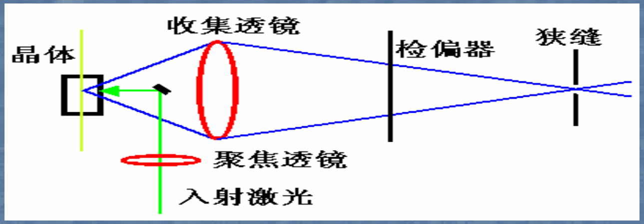

180 °

$x(zz)\bar{x}; x(zy)\bar{x}; x(yy)\bar{x}$

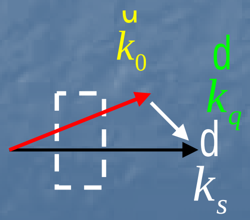

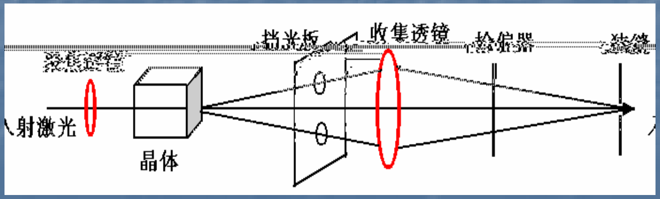

0 °

$y(zz)y; y(zx)y; y(xx)y$

3.3

a:

$\nu_s < \nu_0$

$$\nu_s = \nu_0 - \nu_q$$

d d d

$$k_s = k_0 - k_q$$

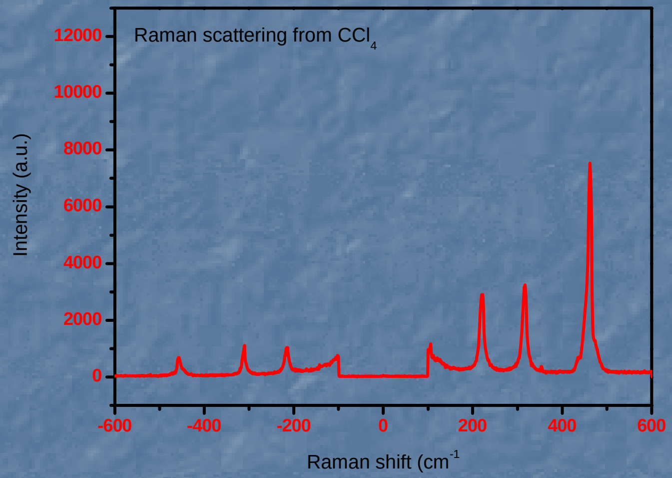

$\nu_s > \nu_0$

$$\nu_s = \nu_0 + \nu_q$$

d d d

$$k_s = k_0 + k_q$$

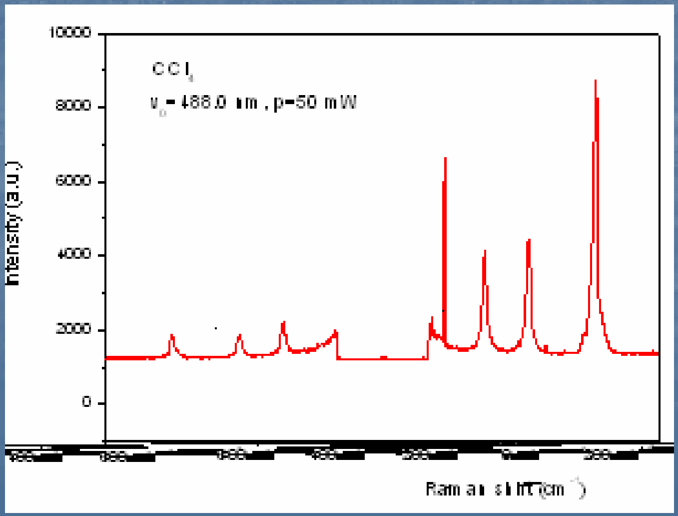

b.

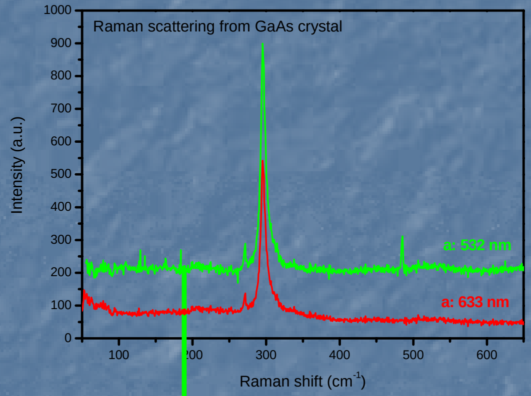
Raman scattering from GaAs crystal
Intensity (a.u.)
Raman shift (cm^{-1})
a: 532 nm
a: 633 nm
0
100
200
300
400
500
600
700
800
900
1000

GaAs

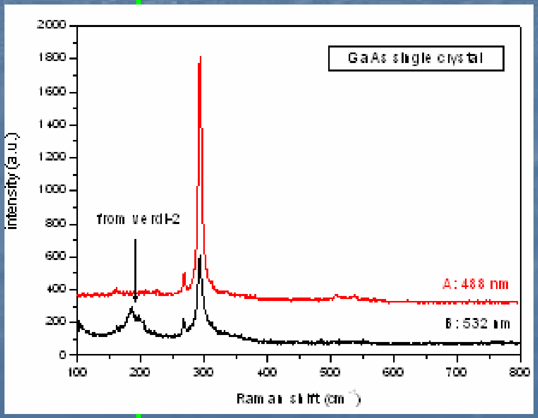
GaAs single crystal
from verdi-2
A: 488 nm
B: 532 nm
Intensity (a.u.)
Raman shift (cm^{-1})

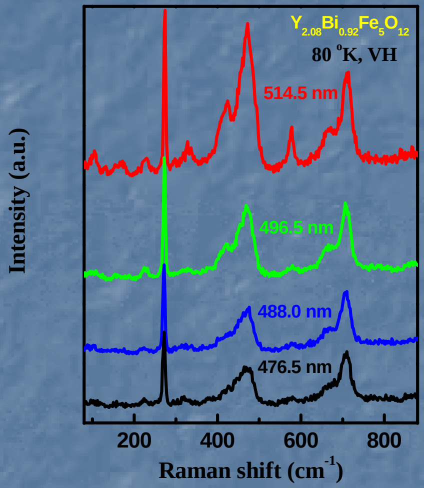
$Y_{2.08}Bi_{0.92}Fe_5O_{12}$
80 °K, VH
514.5 nm
496.5 nm
488.0 nm
476.5 nm
Intensity (a.u.)
Raman shift (cm^{-1})
200
400
600
800

Bi-YIG

c.

Boltzmann

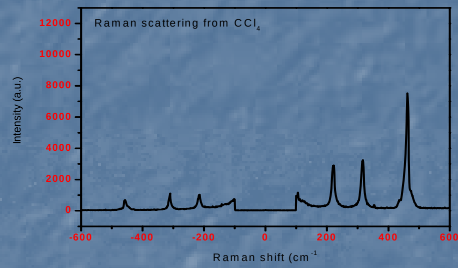

Stokes

$$R=\frac{d\sigma}{d\Omega}\bigg|_{A_s}\Big/\frac{d\sigma}{d\Omega}\bigg|_{S}=\frac{n(\omega)}{n(\omega)+1}=\frac{1}{e^{h\nu/kT}}$$

$$n(\omega)=\frac{1}{\exp\frac{h\nu}{k_BT}-1}$$

Stokes

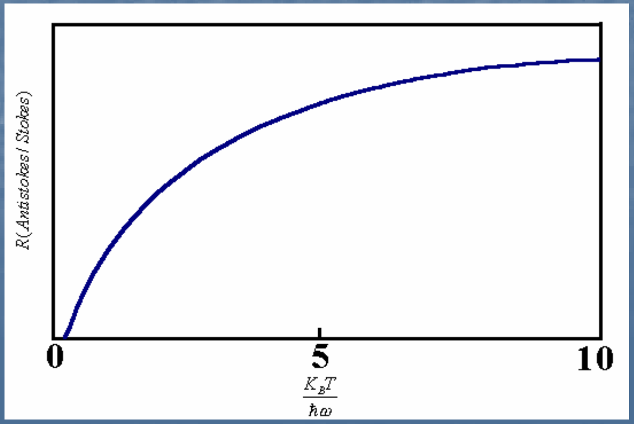

R

CCl_4)

100 mW CCl_4 460 cm^{-1}

Stokes 2063522 counts 250368 counts

$$R = \frac{d\sigma}{d\Omega}\bigg|_{A_s} / \frac{d\sigma}{d\Omega}\bigg|_{S} = \frac{n(\omega)}{n(\omega)+1} = \frac{1}{e^{h\nu/kT}}$$

$$T = -\frac{h\nu}{k_B \ln(I_{AS}/I_s)}$$

$$= -\{(6.63x10^{-34}x4.6x10^{2}x30x10^{9})/[1.38x10^{-23}x(-2.11)]\}$$

$$= 914.94/2.91$$

$$= 314.4(K)$$

$$h = 6.63x10^{-34}JS; k_B = 1.38x10^{-23}J/K$$

3.4

k ≠ 0

$$I(\omega) \propto \int_0^1 \exp(-\frac{k^2L^2}{4}) \frac{dk^2}{[\omega-\omega(k)]^2+[\Gamma_0/2]}$$ **3-9**

ω *k* *L*
L Γ_0

$$\omega(k) = A + B\cos(\pi k)$$ **3-10**

(3-9) (3-10) L Γ

Si

Si

1 Lorentz

2

3 Γ $1/\tau$,

4

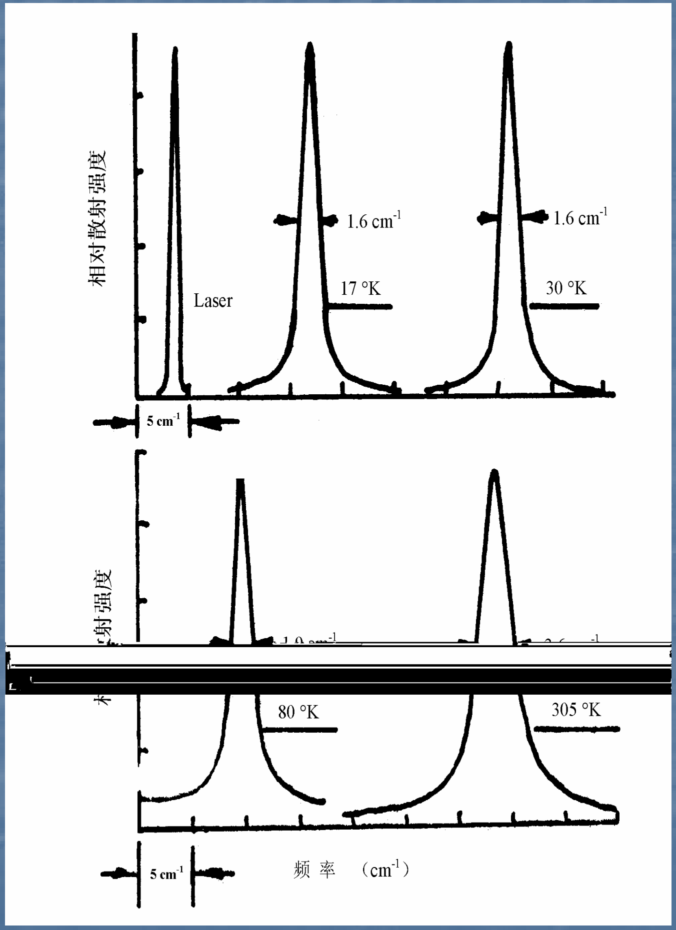

Si

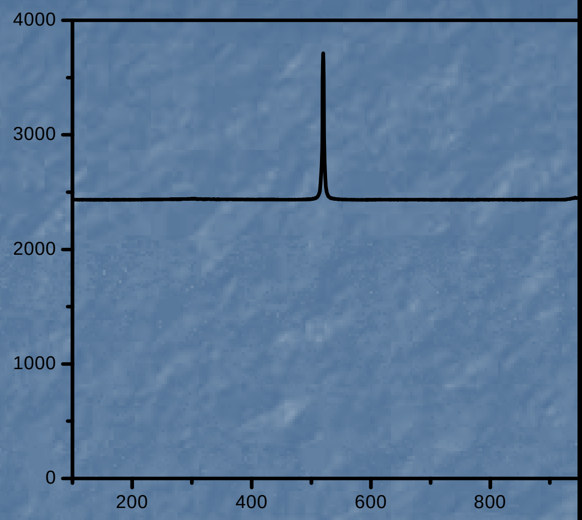

GdS

1 0.8 GdS

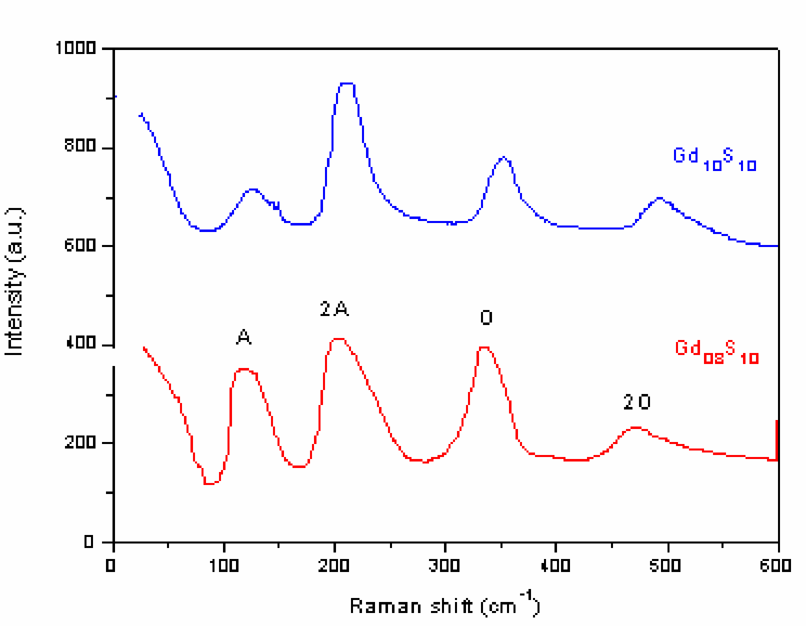

GdS

SnO_2 *P*

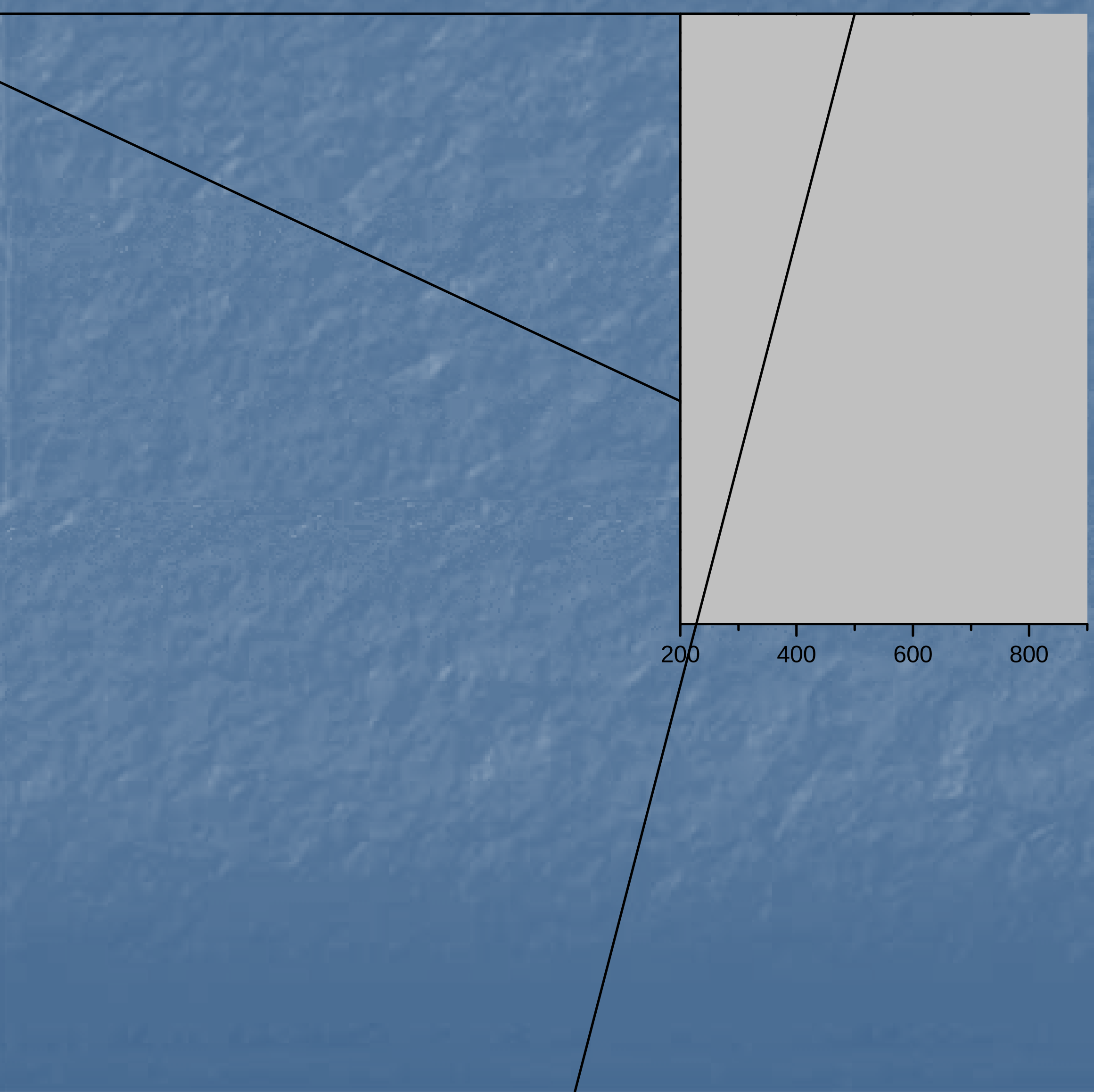

SnO_2

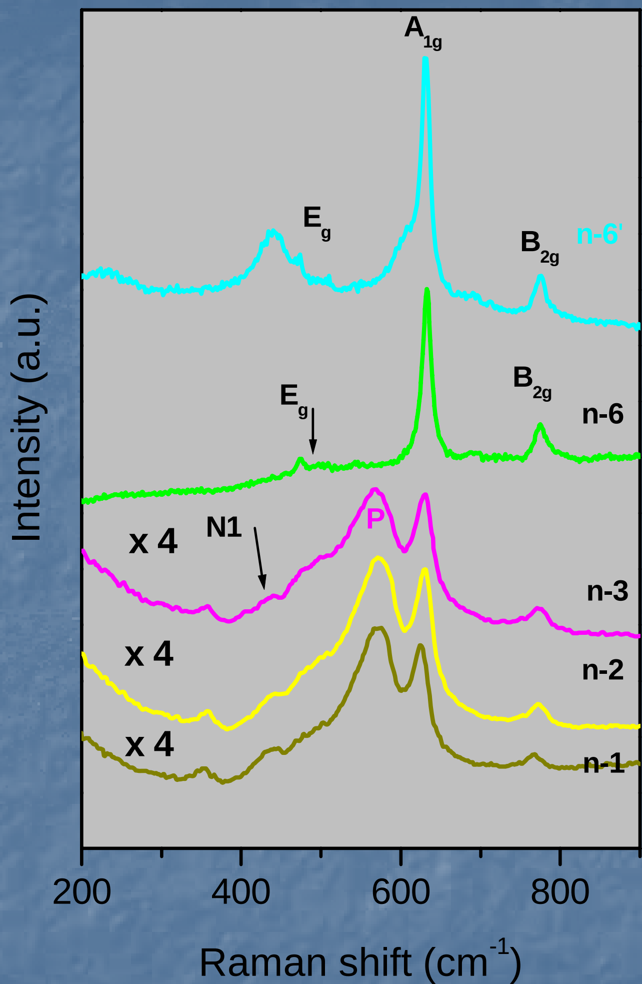

A1g
Eg
B2g
n-6'
Eg
B2g
n-6
x 4
N1
P
n-3
x 4
n-2
x 4
n-1
Intensity (a.u.)
200
400
600
800
Raman shift (cm-1)

N_i)

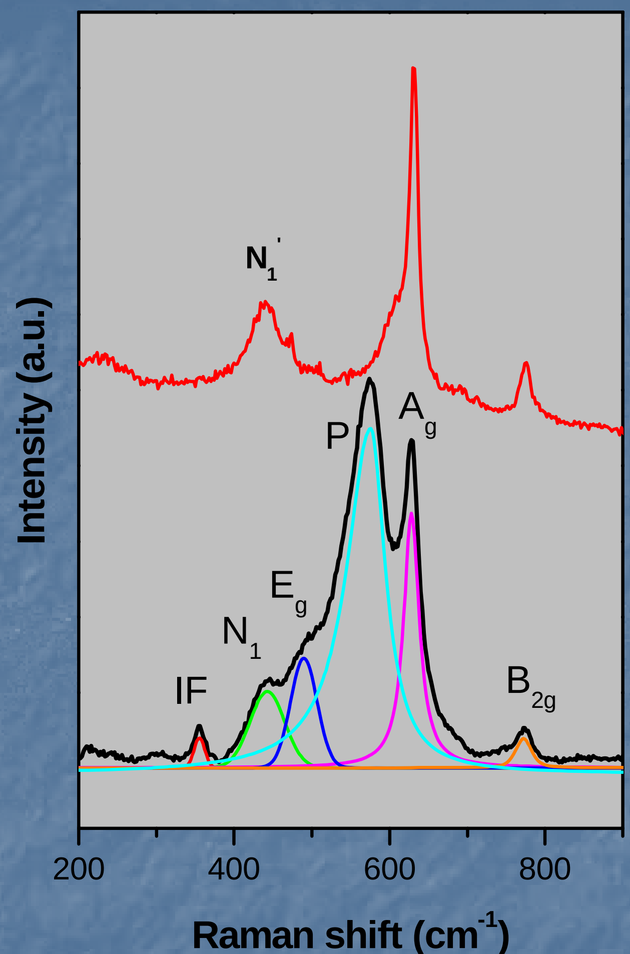

N1'
P
Ag
Eg
N1
IF
B2g
Intensity (a.u.)
200
400
600
800
Raman shift (cm-1)

1.

2

3

4 NH_4Br

1

2

3

4

5

/

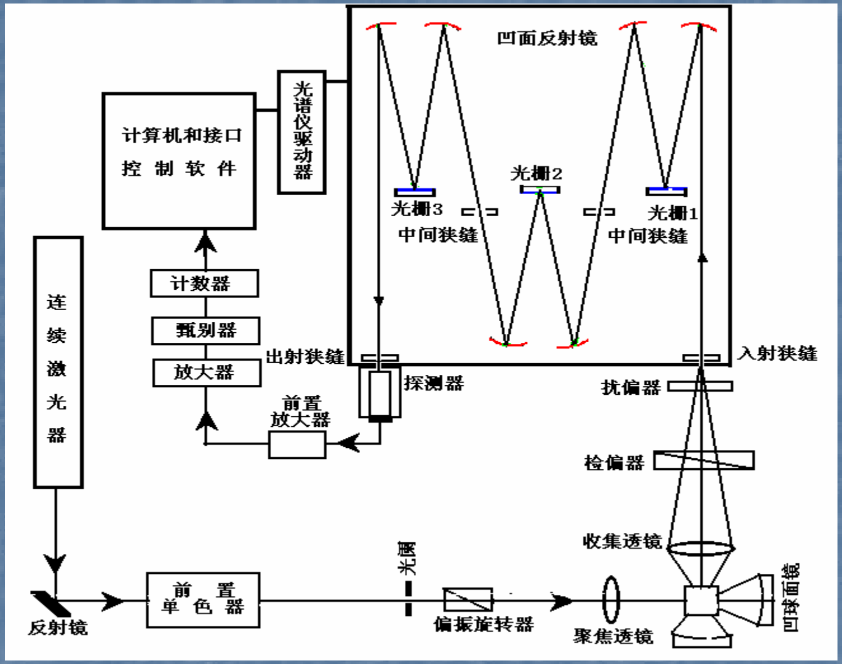

凹面反射镜
计算机和接口
控 制 软 件
光谱仪驱动器
光栅2
光栅3
中间狭缝
光栅1
中间狭缝
计数器
甄别器
放大器
出射狭缝
入射狭缝
探测器
抗偏器
前置
放大器
检偏器
连续激光器
收集透镜
光阑
前 置
单 色 器
反射镜
偏振旋转器
聚焦透镜
凹球面镜

Laser line rejection – Notch Filters

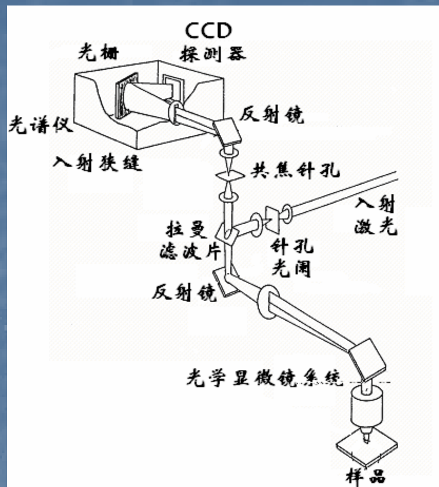

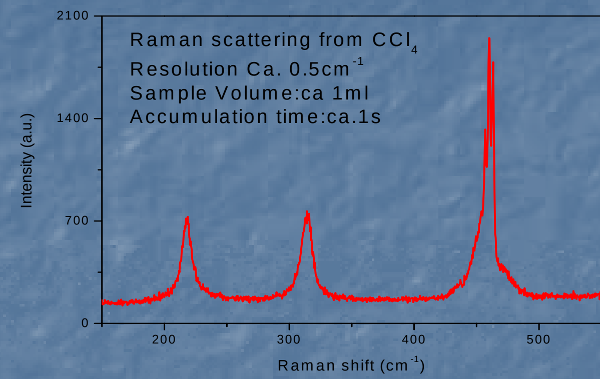

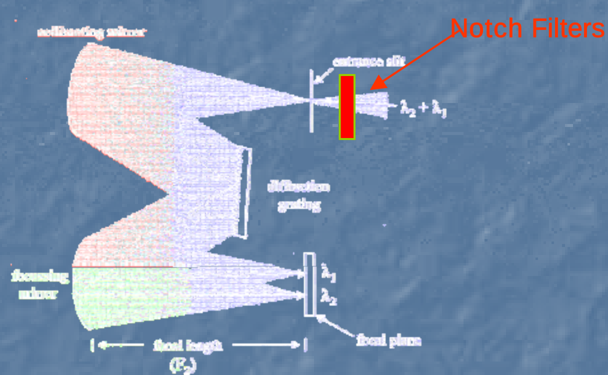

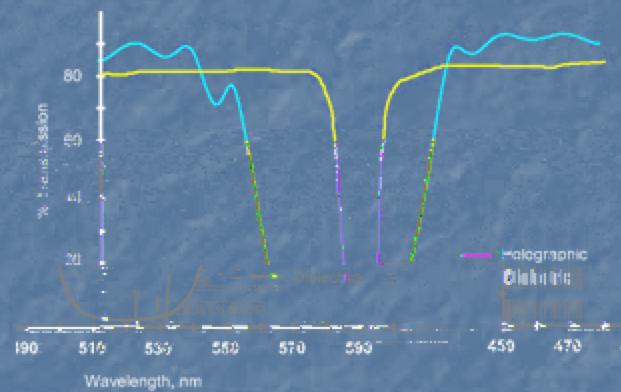

1 2

3 4

1 2

3

Spectrometer – Triplemonochromator

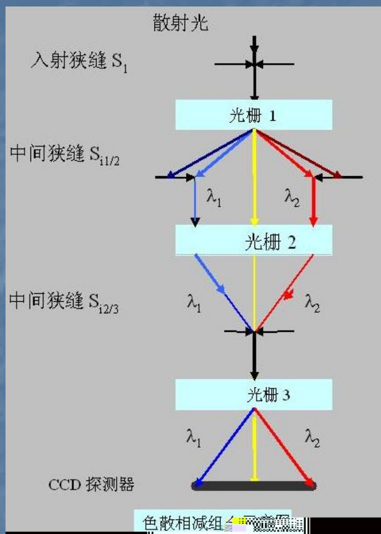

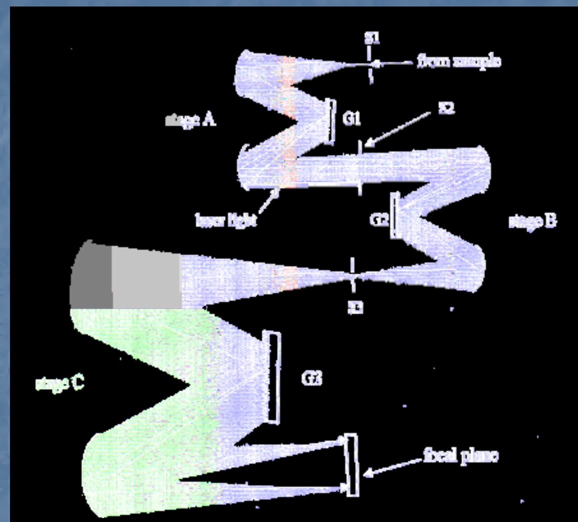

1

2

3

4

5 /

6 CCD/PMT

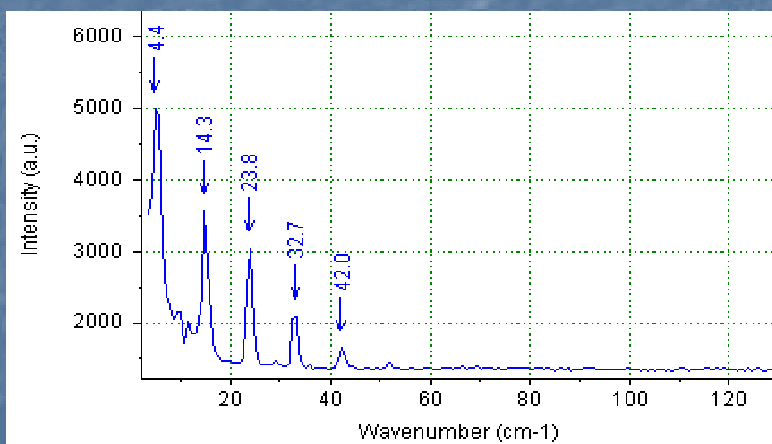

SiGe

Fabry Perot FP

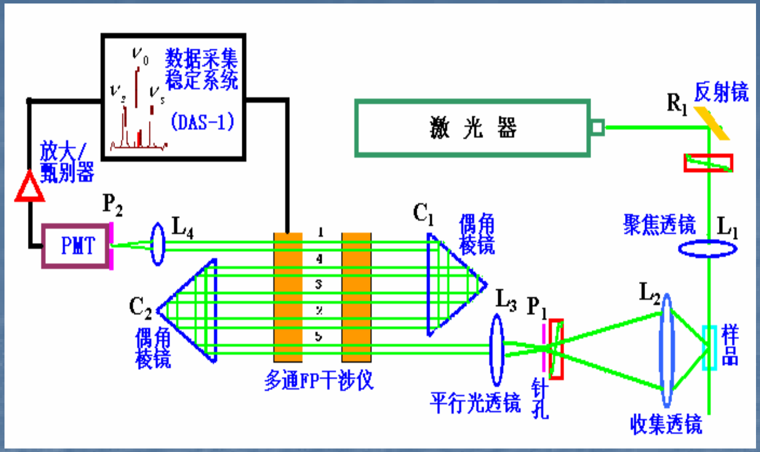

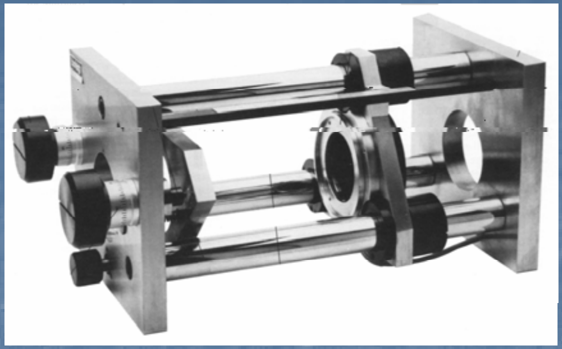

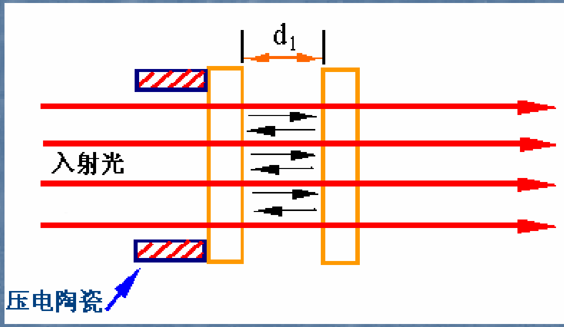

$$m\lambda = 2\, n d_1 \cos\theta$$

(FSR)

$$FSR = C \quad /2d_1$$

(F,)

$$F = FSR / \Delta\nu$$

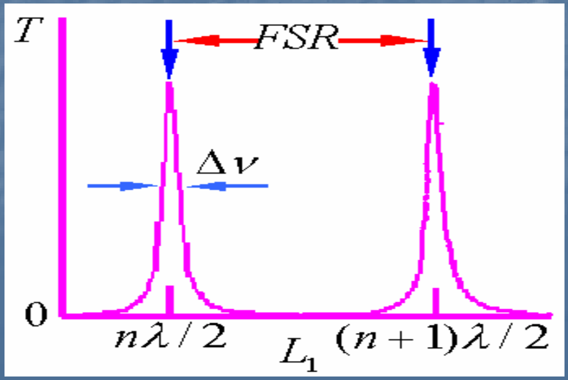

$$C = I_{max.} / I_{min.} \approx 4F^2 / \pi^2 \leq 10^5$$

Dr. J.R.Sandercoker F-P

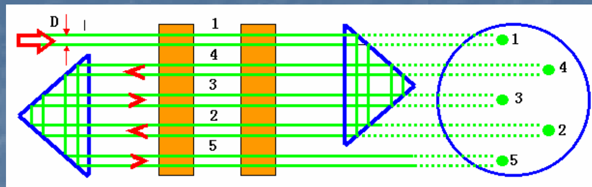

FP

FP

$$C_p = C_1^p$$

FP

$$F_p = (2^{\frac{1}{p}} - 1)^{-\frac{1}{2}} \cdot F_1$$

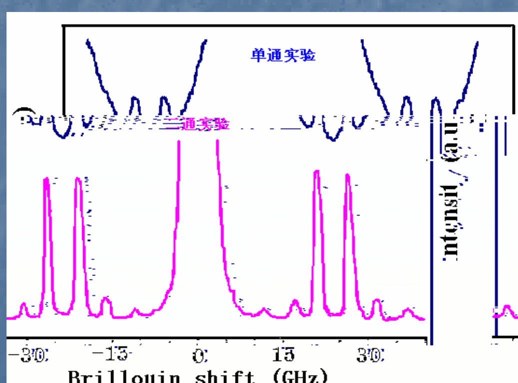

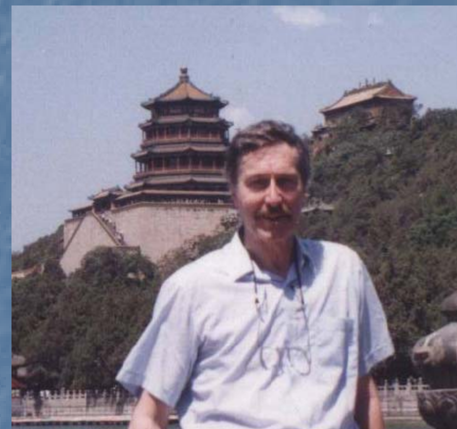

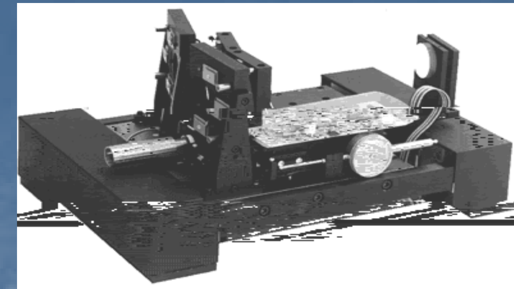

FP

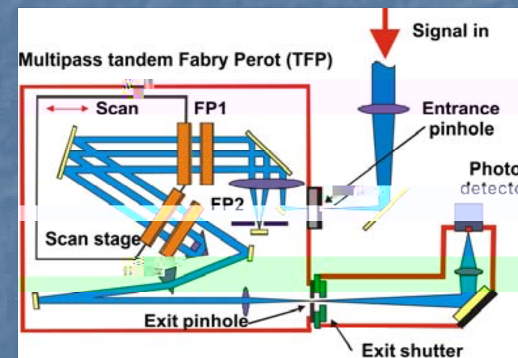

FP

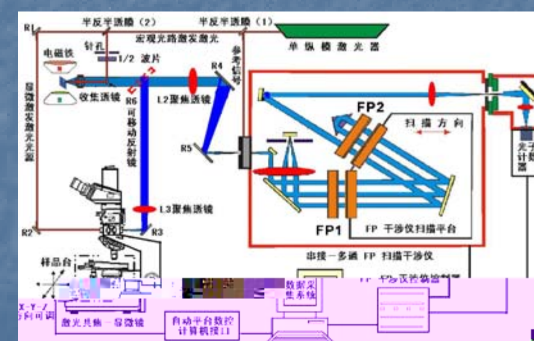

(ν), (I), (Γ)

Light Scattering from Magnons and Phonons in $Y_{3-x}Bi_xFe_5O_{12}$ (Bi-YIG) Single Crystals

1. Bi-YIG structure and their applications
2. Brillouin light scattering from Bi-YIG crystals
3. Raman scattering from Bi-YIG crystals
4. summary

The crystal structure of $Y_{3-x}Bi_xFe_5O_{12}$

Yttrium iron garnets of the composition $Y_3Fe_5O_{12}$ (YIG), which is a typical ferrimagnet, have been important to microwave and magneto-optic technology.

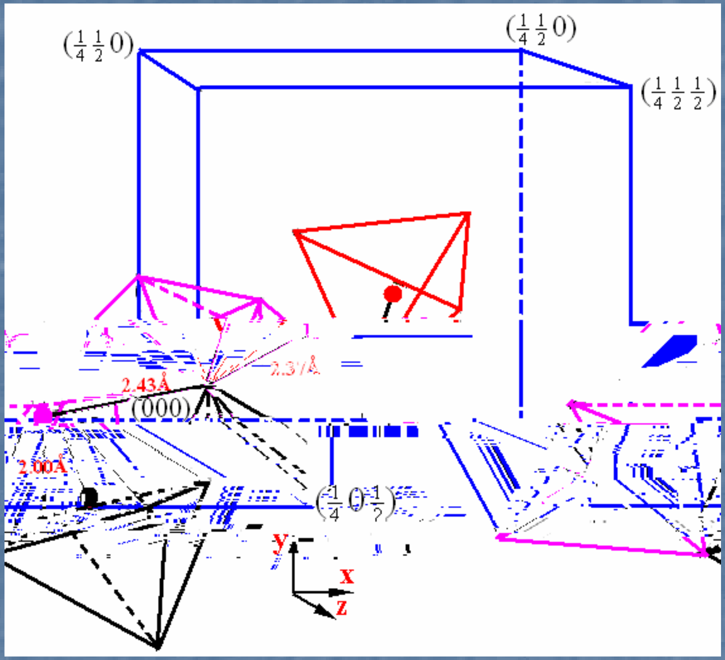

The structure of $Y_3Fe_5O_{12}$

$\{Y_3\}^c[Fe_2]^a(Fe_3)^d O_{12}$ (YIG)

doping Bi^{3+}

$\{Y_{3-x}Bi_x\}^c[Fe_2]^a(Fe_3)^d O_{12}$ (Bi-YIG)

- Fe^{3+} (octahedral, a sites)
- Fe^{3+} (tetrahedral, d sites)
- Y^{3+} (dodecahedral, c sites)

The Faraday rotationθ_F and Keer rotationθ_K, as well as the Curie temperature,of Bi-YIG increase with the Bi concentration.

Bi-YIG

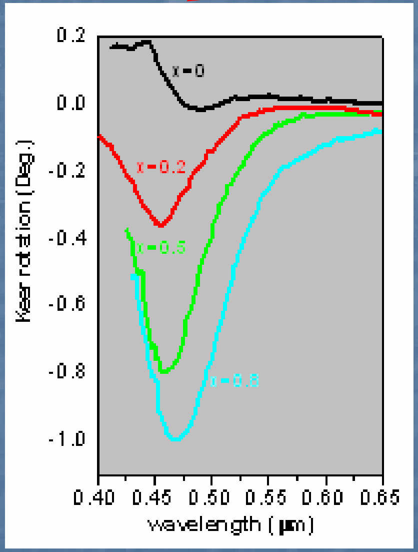

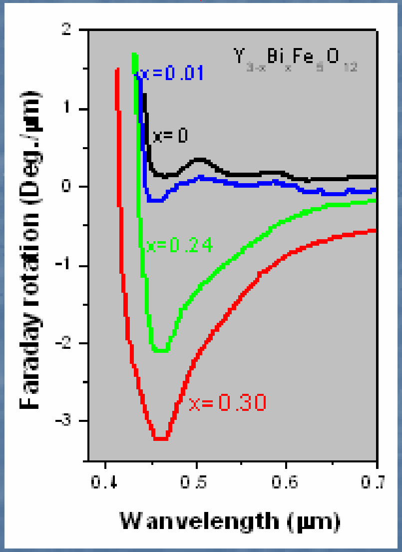

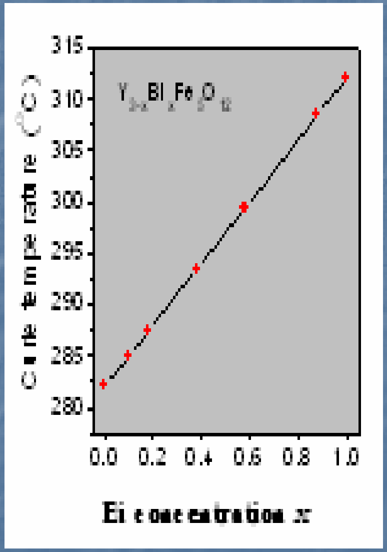

The magneto optic –enhanced effects on Bi-YIG have attracted considerable experimental and theoretical interest in the past, various mechanism of the effects proposed. The physical origins of these effects are not clear so far. Thorough theoretical and experimental description to their origins is still needed.

Mainly different opinions:

1. **New type of transitions in Bi-YIG have been appeared**

Experiment: samples and their compositions

Bi-YIG single crystals were grown by the flux method. The melt of constituent oxides with Bi_2O_3-PbO-B_2O_3 as flux was slowly cooled in Pt crucible.

Five slab samples cutting from bulk crystals with x=0, 0.14, 0.36, 0.54 and 0.92, respectively, all of size ~2.0x2.x0.5mm^3, are selected for Brillouin light scattering.

Experiment: equipments and scattering geometry

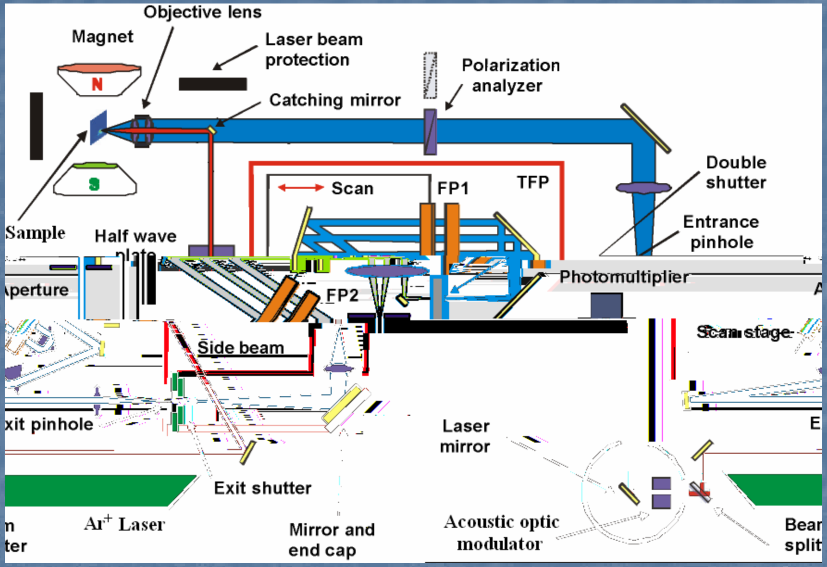

A JRS tandem Fabry-Perot interferometer

(3+3 systems) for BLS

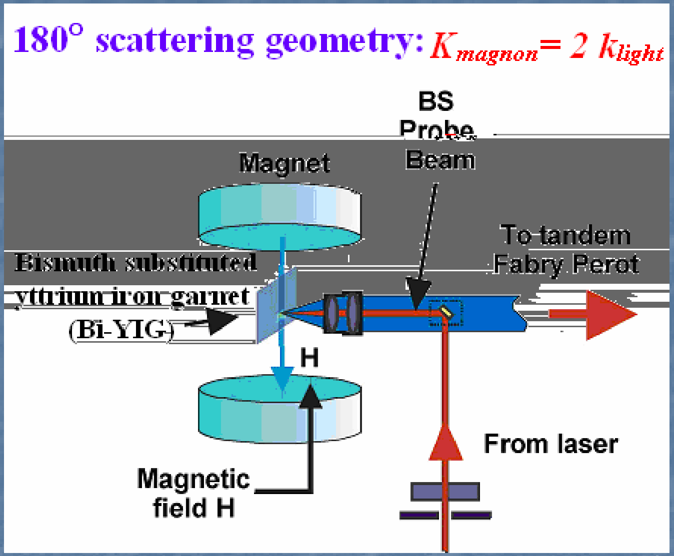

Back scattering: The optic axis of a focusing and collecting lens is taken to be the x axis. The sample slab stands vertically on the holder in the gap of a magnet and its surface normal coincides with the axis.

The broadening and downshift effect of laser power on magnon

When laser power exceeds 25 mW, the spectra deteriorate drastically: the peaks weaken and widen markedly with decreasing frequency shift and intensifying anti-symmetry. It shows that large-power excitation could affect the magnetic order of the crystal Bi-YIG and produce widening of spectral lines.

Low power of 5 mW was used and the results were good.

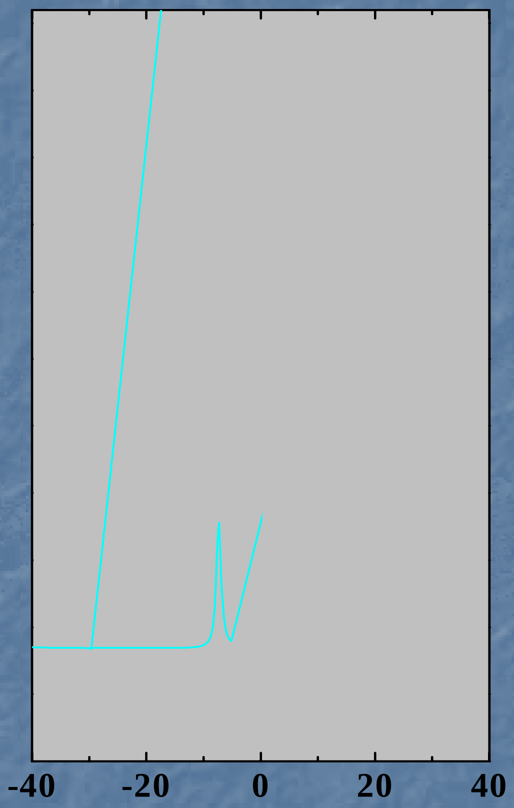

Effect of Bismuth concentration on sound velocity

The LA sound velocity V_L:

;

V_L =7.18x10^5 cm/s for YIG

V_l =6.71x 10^5 cm/s for Bi-YIG (x=0.54)

…and the band width of bulk magnons

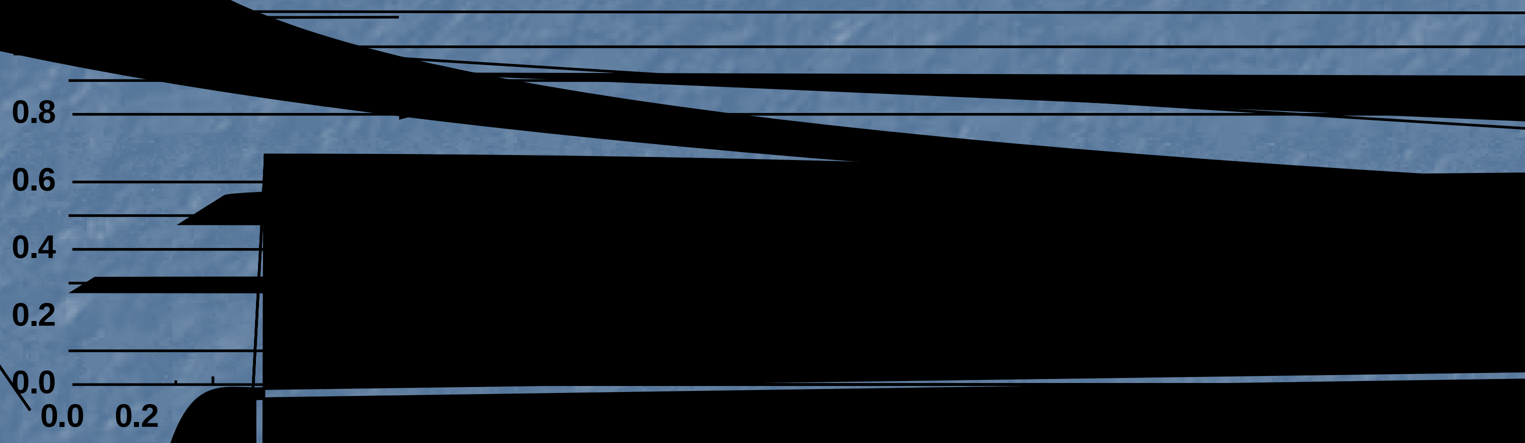

Bi-concentrat…
bulk-magnon…
linewidth (tr…

Polarized BLS spectra of magnons from Bi-YIG as the external magnetic field H_0.

(a) Bi-YIG (x=0.92)

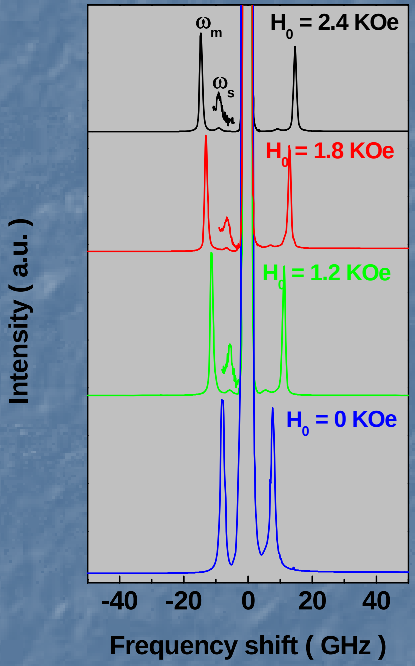

(b) Bi-YIG (x=0.54)

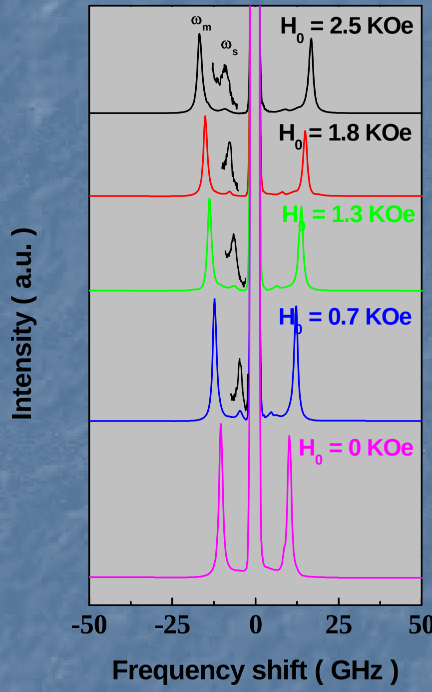

ω_s is determined to be scattering from magnon too by varying external field and scattering polariztion.

The stiffness constant D_{ex} in Bi-YIG

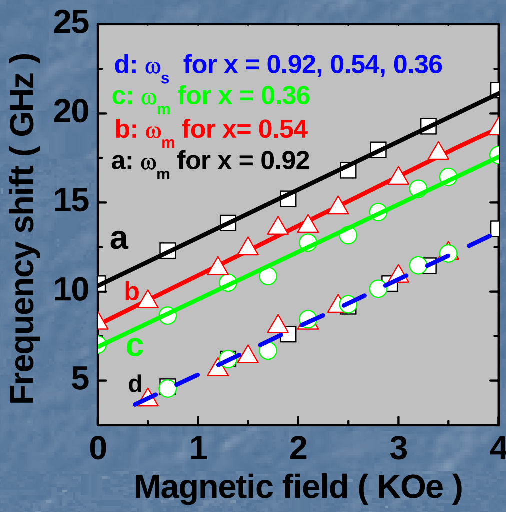

Magnetic-field dependence of the bulk magnons frequencies ω and the weak peaks in Bi-YIG at 514.5 nm excitation. The squares, triangles, circles are data for x=0.92, 0.54,and 0.36,respectively, the solid lines are fited from Eq.(2)

The magnon frequency ω_m should be related to the effective magnetic field H_0 and the magnon wavevectork_m, for $k_m \perp H_0$, by the dispersion relation:

$$\omega_m = \gamma^2 \sqrt{(H_0 + D_{ex} K_m^2)(H_0 + D_{ex} K_m^2) + 4\pi M_s} \qquad (1)$$

γ is the gyromagnetic ratio, H_0 should the external field and both the anisotropic field and demagnetizing field ($H_0 = H_{appl.} + H_{an} + H_{demag.}$) . D_{ex} is the spin wave exchange stiffness constant and $4\pi M_s$ is the saturation magnetization. D_{ex} and $4\pi M_s$ are taken as parameters fitted to the experimental data.

The dispersion relation for our experiment:

$$\omega_m \approx \gamma [H_0 + D_{ex} K^2 + (1 - 2N) 2\pi M_s] \quad (2)$$

TABLE 1. The stiffness constant D_{ex} and saturation magnetation $4\pi M_s$ in Bi-YIG

Concentration	Stiffness Constant $D_{ex}/10^{-9}$ Oe cm^{-2}			Saturation Magnetization $4\pi M_s/G$	
x	5 mW	25 mW	30 mW *	5 and 25 mW	30 mW *
0.00	5.58	5.40	5.4	1753	1750
0.14	6.03	5.87	5.9	1760	1756
0.36	6.48	6.23	6.2	1766	1762
0.54	6.98	6.75	6.7	1773	1770
0.92	8.06	7.66		1792	

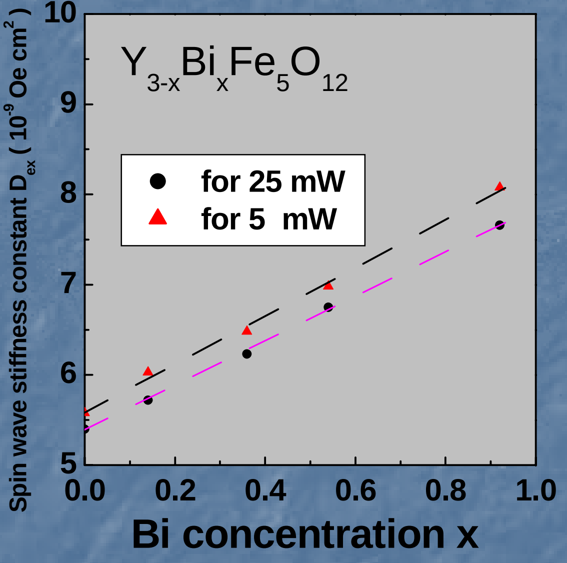

Bi-concentration dependence of the spin-wave stiffeness constant D_{ex} under 5 and 25 mW, respectively.

New weak peak ω_s in Bi-YIG

1. Could it be a surface magnon? 2. Could it be a kind of density-states effects of magnon ?

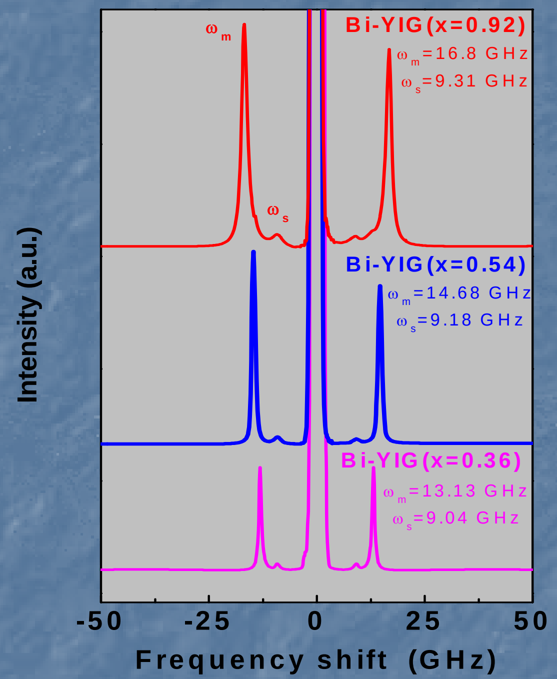

BLS spectra of the bulk magnon ω_m and weak peak ω_s for different Bi concentration in exteral magnetic field of 2.5 kOe.

BLS spectra of magnons of Bi-YIG (x=0.92) at 457.9 nm (θ_i=20°;H =3.3 kOe) and 514.5 nm (θ_i=20°, 60°; H =3.3 kOe) excitations, respectively

The frequency of surface magnon ω_s could be determinted according to the theory of surface magnon.

Magnetic-field dependence of the weak peaks in the Bi-YIG at 514.5 nm. The squares, triangles, and circles are data for x= 0.92, 0.54,and 0.36 . The dash line is fitted from the formula.

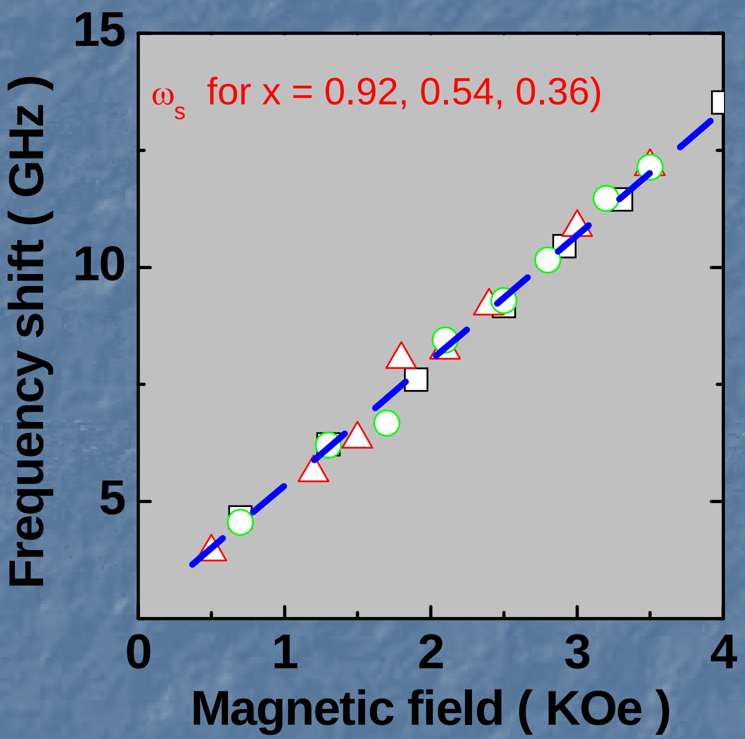

$$\omega_s = \gamma\sqrt{H_0(H_0 + 4\pi M_s)}$$

3. Raman scattering from Bi-YIG crystals

The enhancement of the magneto-optic coupling owing to The Bi-doping makes an opportunity of optic magnon in the magnetic materials.

The result will provide useful information for studying the relationship between the Bi concentration, the microstructure of Bi-YIG crystals, and their magnetic and mechanical properties if the magnon is found.

The crystal structure of Bi-YIG and Raman active phonons:

The crystal structure of Bi-YIG belong to the space group O_h^{10} (Ia3d), isomorphic to that of YIG. Since contains the inversion operator, the *K* = 0 phonons are either infrared active ,Raman active, or silent. There are 25 Raman active phonons which can be classified as 3A1g + 8Eg + 14T2g

Crystal orientation and selection rules

Polarized Raman spectra of Bi-YIG with Bi-concentrations x = 0, 0.14, 0.36, 0.54 and 0.92 at room temperature using 514.5 nm argon emission

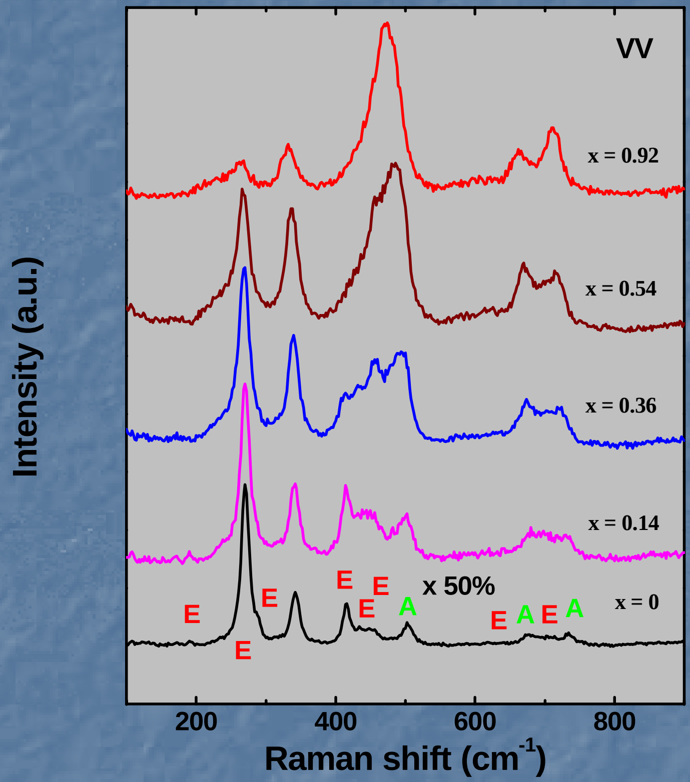

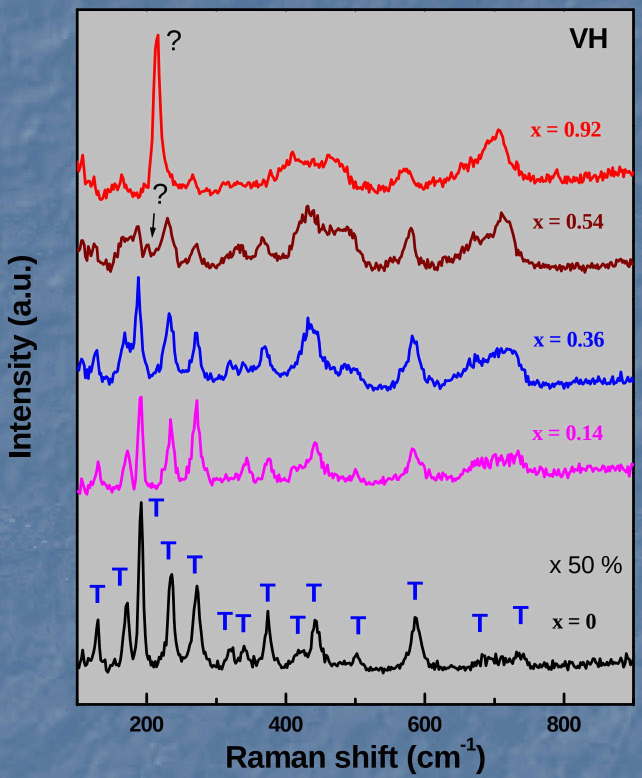

What is the new peak in Bi-YIG(x= 0.54, 0.92) ?

Raman spectra of Bi-YIG (x=0.92)with four different laser lines at 100 °K

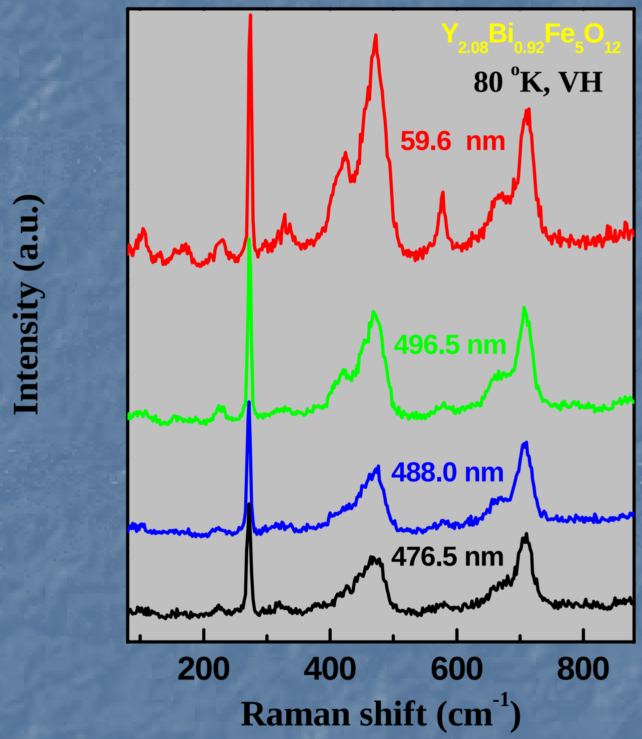

Raman data were taken with four different laser lines from argon laser, in order to eliminate misidentification of our Raman data duo to possible fluorescence from trace impurities.

Finally, the observed process is indeed a first order scattering rather than a fluorescence was confirmed by observing the anti-Stokes line at 40 ° K, where $Z\omega / kT \approx 2$.

Could it be a electronic Raman scattering or optical magnon?

Polarized Raman spectra of Bi-YIG (x=0.92)measured at various temperatures between RT and 10 ^{o}K in VV and VH scattering geometry

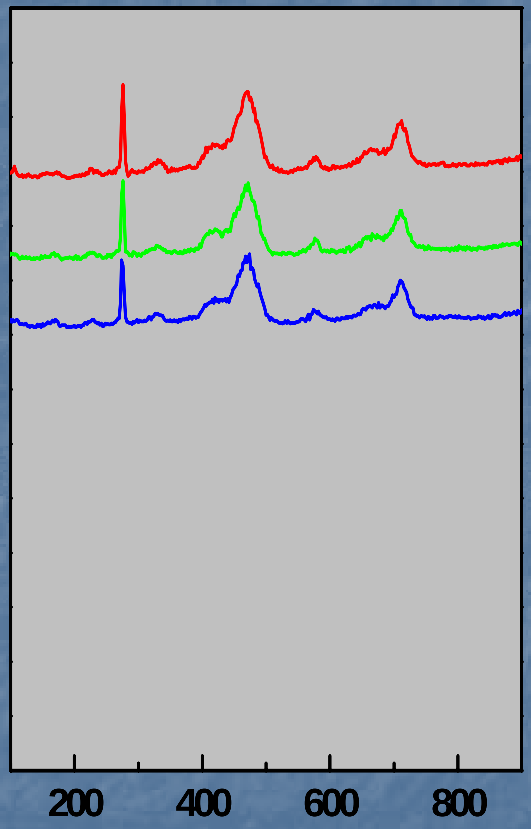

Polarized Raman spectra of Bi-YIG(x=0.92) measured at higher temperatures in VH scattering geometry

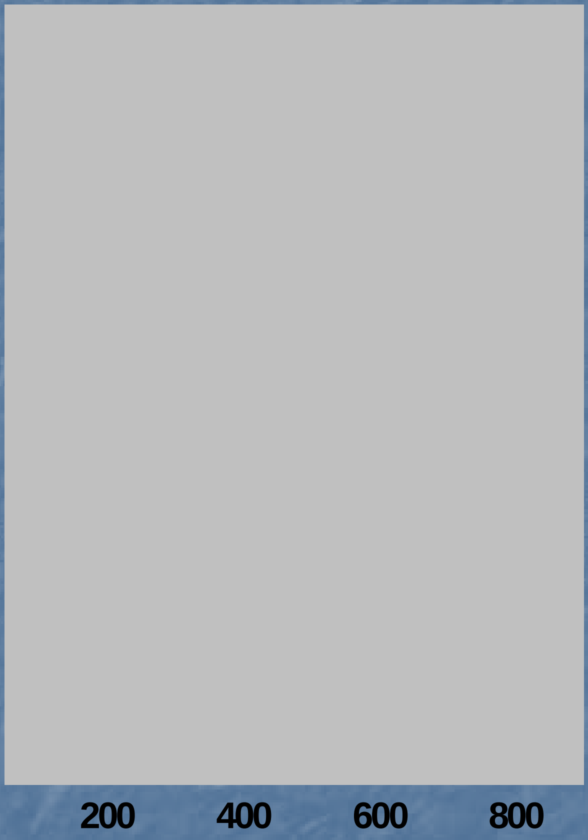

Polarized Raman spectra of Bi-YIG (x=0.54)measured at various temperatures between RT and 10 ^{0}K in VV and VH scattering geometry

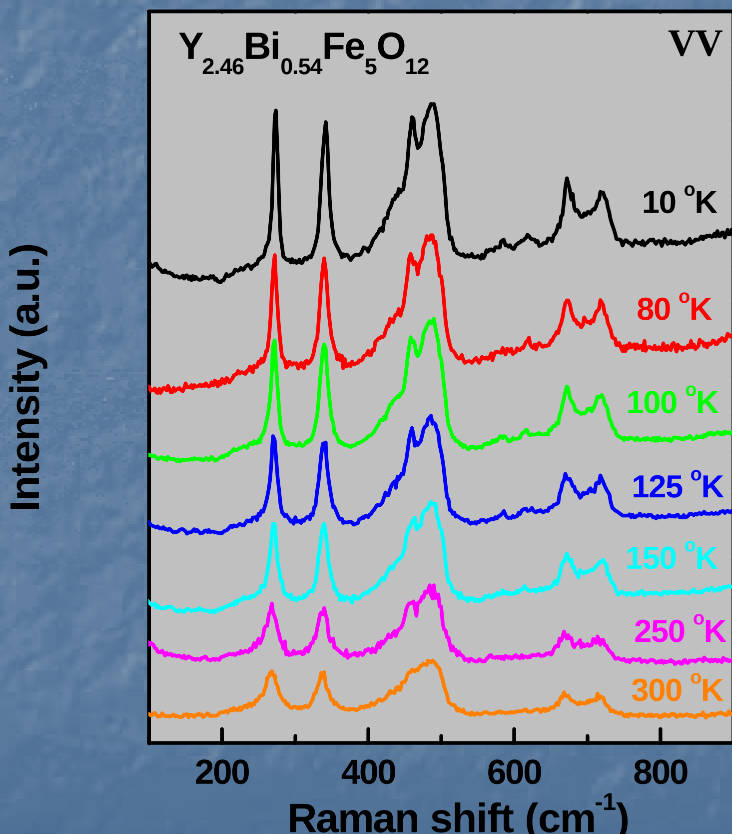

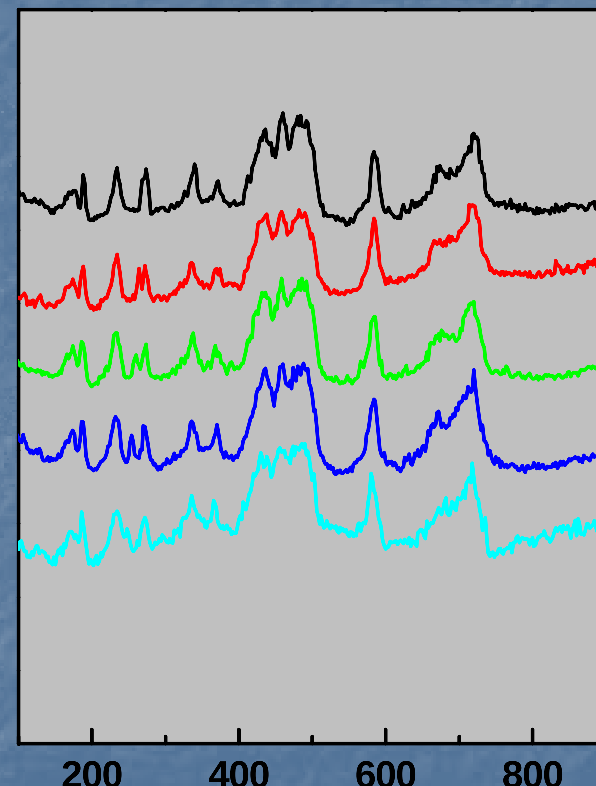

Temperature dependence of Stokes frequency shifts in Bi-YIG (x=0.92)

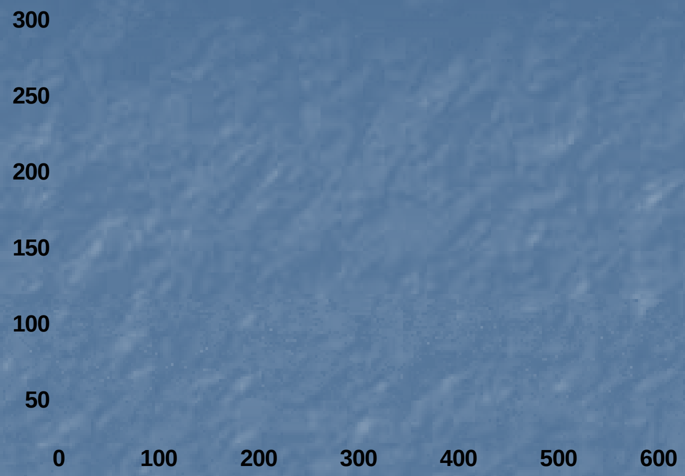

Approximative calculation of the exchange resonance magnon

The exchange resonance frquency between two sublattice was derived by Kaplan and Kittel

$$\omega_m = \lambda(\gamma_2 M_1 - \gamma_1 M_2) \qquad (1)$$

where is λ the molecular field constant; $\gamma_{1,}\gamma_2$ the respective gyromagnetic ratios; and $M_{1,} M_{2;}$ the sublattice magnetizations.

$$\omega_m = \gamma H_{E,} \qquad (2)$$

$H_E = \lambda M(t)$ is the exchange field . M is the average sublattice magneization. λ can be calculated from the experimentally measured quantities.

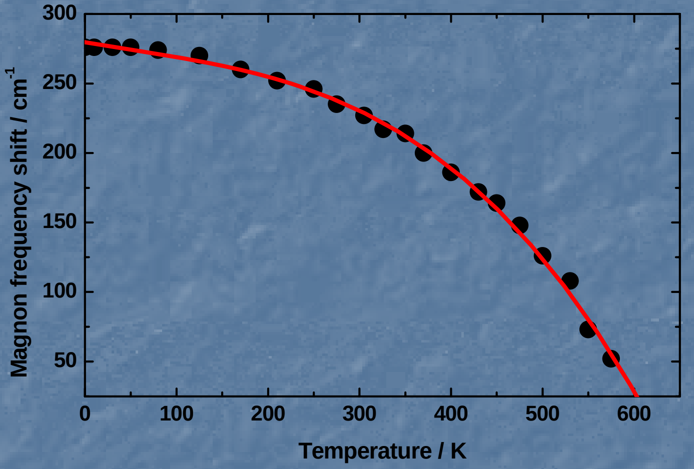

Raman scattering from {$Bi_{1.4}Ca_{1.6}$}[Fe_2]($Fe_{2.2}V_{0.8}$) single crystal

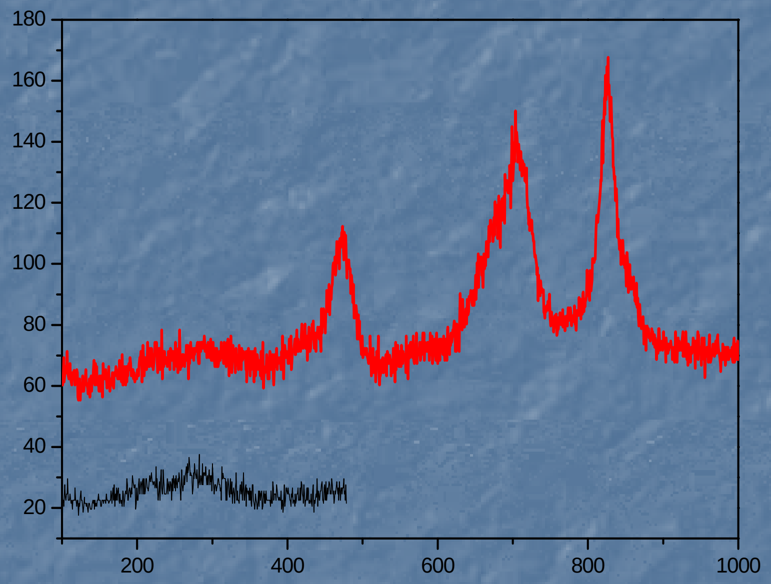

The substitution Y with Bi decreases the intensity of Raman shift in the range of the lower frequency .

The appearance of the exchange resonance magnon not only depends on the Bi concentrations in the crystal but also on the exchange interaction between the octahedral sites and tetrahedral sites.

Summary

1. In BLS, the spin wave exchange stiffeness constant $D_{ex}$is very sensitive the excitation power so that low power should used.
2. The behavior of the bulk magnon is opposite to LA phonons.
3. Not only the spin wave exchange stiffness constant, but also the relative intensity and the bandwidth of bulk magnon increase linearly with x.
4. The substitution Y with Bi softens the crystals and the measured sound velocities of the acoustic phonons decrease linearly with x.
5. As an external field is applied, the uniform magnetostatic mode appears.
6. In Raman scattering, the exchange resonance magnons are firstly observed in Bi-YIG($x > 0.54$).

Summary

7. The appearance of the exchange resonance magnon not only depends on the Bi concentrations in the crystal but also on the exchange interaction between the octahedral sites and tetrahedral sites.

Tha